*Thermochimica Acta*, 55 (1982) 75–87
Elsevier Scientific Publishing Company, Amsterdam—Printed in The Netherlands



# CHARACTERIZATION OF THE CALCINATION PROCESS OF YTTRIA

KAN-SEN CHOU * and LAWRENCE E. BURKHART

*Ames Laboratory, USDOE, Iowa State University, Ames, IA 50011 (U.S.A.)*

(Received 6 November 1981)

## ABSTRACT

A complete characterization of the calcination of precipitates obtained from a continuous operation was carried out in this study. The precipitate was obtained by reacting yttrium nitrate and ammonia solutions in a MSMPR reactor. It precipitated out as yttrium hydroxide nitrate hydrate, which has the general form $Y_2(OH)_{6-x}(NO_3)_x \cdot y\ H_2O$. This compound decomposed in consecutive steps with the last reaction occurring at 525°C.

The calcination process was characterized by chemical analysis, X-ray diffraction analysis, DTA and TG. In addition, the physical characteristics of calcined powders, such as specific surface area, particle size distribution, pore volume distribution, X-ray crystallite size and conversion were measured as a function of calcination temperature and time. Finally, the kinetics of the reduction of surface area, the growth of crystallite size and conversion were also examined.

## INTRODUCTION

The production of ceramic powders has been for centuries based on the experience of the operators instead of on the results of rigorous scientific studies. With the stringent property requirements for new high-performance ceramics, it is necessary to have better control over the preparation processes. As always, the first step toward such a goal is to understand the mechanism of the processes and to relate the properties of the products to appropriate parameters.

In a conventional ceramic fabrication process, calcination has always been one of the major steps in powder treatment before the sintering one. Although calcination is an important step in powder preparation, few systematic studies [1–5] have been made about its effects on powders. This led to the present study of the calcination of yttria. The composition, morphology, size distribution, surface area and other properties of the calcined powders were thoroughly characterized and related to different calcination conditions. This complete characterization process will enable

* Present address: Department of Chemical Engineering, National Tsing Hua University, Hsinchu, Taiwan, ROC.

us to understand not only the changes during calcination but also its relationship with other steps such as precipitation, drying and sintering in the ceramic fabrication process.

## EXPERIMENTAL

### *Material*

Yttrium hydroxide nitrate hydrate powder was obtained by reacting yttrium nitrate solution with ammonia in a continuous MSMPR reactor [6]. After filtration and washing with water, the precipitate was washed with acetone, toluene and acetone as described by Hunter et al. [7]. Powder from several precipitation runs carried out under various conditions were then mixed well and used as the starting material in this study.

### *Calcination runs*

The calcination runs were done in a box type muffle furnace. Small crucibles of 30 ml were used. The depth of samples in the crucible was kept at about 1 in throughout the study. Crucibles were put into the furnace before it was turned on. The heat-up curve is shown in Fig. 1. The time count was started as soon as the temperature reached the desired value. Symbols, such as 775-0 and 775-1, mean that the samples were taken out of furnace immediately the temperature reached 775°C, and one hour later, respectively.

For qualitative X-ray work and chemical analysis, the calcination runs were made in a different way. Five crucibles were initially put into the furnace. The furnace was then set at 250°. After one hour at this temperature, the first sample (called X-250) was taken out and the temperature was raised to 350°. It was held there for another hour before the second sample (X-350) was taken out. This procedure was then repeated at 450, 550 and 900° for the third, fourth and fifth samples.

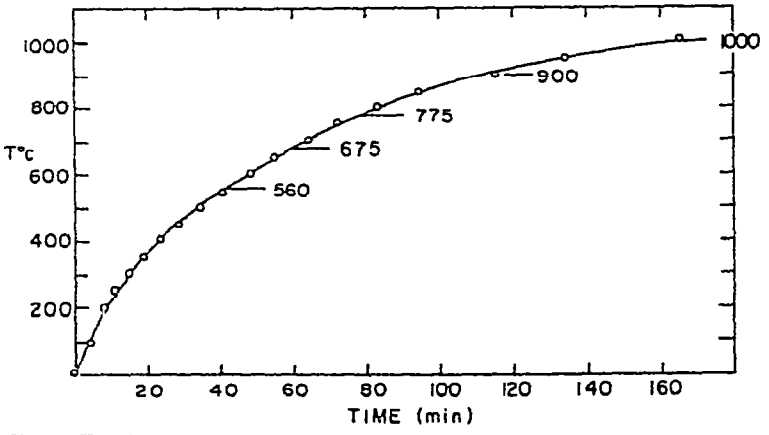


Fig. 1. The heat-up curve of the muffle furnace used in this study.

*Qualitative analysis*

In order to characterize the qualitative aspects of the calcination reactions and their products, the following methods were employed.

(a) Chemical analysis for yttrium and nitrate ion contents in the precipitate and calcined powders.

(b) X-Ray diffraction analysis for any structural changes in the product.

(c) DTA and TG for thermal and weight changes during calcination.

*Powder characterization*

For powder characterization, the following properties of the calcined products were measured: surface area, pore size distribution, particle size distribution, X-ray crystallite size and conversion.

Nitrogen adsorption and desorption isotherms were measured for the analysis of surface area and pore size distributions. All samples were outgassed at 120°C under vacuum overnight before each measurement. The surface area was calculated with the BET equation using a cross-sectional area at 16.2 $Å^2$ for nitrogen molecules.

As to the pore size distribution, the desorption isotherms of nitrogen were used. Through trial and error, it was found that the assumption of a cylindrical pore structure and a Halsey-type expression for the adsorption layer thickness, i.e. $t = 3.19[-5/\ln(P/P_S)]^{0.45}$ would produce the best results, as judged from the difference between the BET surface area and the cumulative surface area obtained from the pore volume analysis.

The particle size distribution of calcined powders was determined by Coulter counter using a 70 micron tube. A 3% solution of LiCl in methanol was used as the electrolyte, and all samples were treated in an ultrasonic bath for exactly 5 min before each measurement.

Finally, a Philips diffractometer, employing Fe filtered Cu K$\alpha$ radiation was used to examine the powder for its X-ray crystallite sizes and degrees of conversion (or crystallization). The slit system consisted of 1° divergence, 0.05° receiving and 1° antiscatter slits, with Soller slits in both the incident and diffracted beams. The (222) or $d = 3.06$ yttrium oxide peak was continuously scanned four to five times for each sample. The half maximum breadths and integrated intensities were then averaged. The reference material used was calcined at 1000°C for 21 h.

The measured half maximum breadths were then corrected for $\alpha_1\alpha_2$ separation and instrumental broadening effects. Both corrections were determined graphically with the help of correcting curves from Klug and Alexander [8], as described by Rosauer and Handy [9]. After these corrections, the X-ray crystallite sizes were calculated by the Scherer equation, assuming $K = 1$. As to the degree of conversion, the integrated intensity was compared directly with that of the reference material, assuming that the latter has been totally converted into crystalline yttrium oxide.

## RESULTS AND DISCUSSION

### *Chemical composition of the precipitate*

It has been shown [10,11] that in the presence of the nitrate ion, yttrium will precipitate out as yttrium hydroxide nitrate instead of the pure hydroxide. Furthermore, a general formula of $Y_2(OH)_{6-x}(NO_3)_x \cdot y\ H_2O$ $(0.5 \leqslant x \leqslant 1.0)$ has been suggested to describe the composition of this compound.

The chemical analysis of this starting material for calcination shows that the $NO_3^-$ / Y ratio is 0.27. Thus, the empirical formula for this precipitate will be $Y_2(OH)_{5.46}(NO_3)_{0.54} \cdot 1.6\ H_2O$.

### *Qualitative analysis of the calcination process*

It has been pointed out [6] that there are two kinds of particles in a precipitate, i.e. crystallites and agglomerates. From the SEM pictures shown in Fig. 2, this is obviously true for yttrium hydroxide nitrate particles. During the calcination process, the chemical composition of the compounds changed consecutively was water and nitrogen components were released from the sample. However, the shapes of the crystallites and agglomerates did not make any significant changes at all, as seen in Fig. 2(b).

Chemical analysis of the calcined products is shown in Table 1. It is very clear from this data set that the nitrate content begins to decrease only above 350°C. By 550°C, most of the nitrate ion has already gone. Nevertheless, traces of nitrate ion will remain in the solid even after calcining at 900°C for one hour.

The DTA and TG curves of the original samples are shown in Fig. 3. Generally speaking, they are very similar to those reported by others [10,12]. There are three endothermic peaks in the DTA curve. Corresponding to each of these peaks, there are significant changes in the TG curve. Combined with the results from chemical analysis, it is not difficult to infer that the first two endothermic peaks on the DTA

TABLE 1

Chemical analysis of calcined samples

| Sample | Y (wt.%) | $NO_3$ (wt.%) | Molar ratio $NO_3^-$ /Y |
|---|---|---|---|
| Original | 51.0 | 9.61 | 0.27 |
| X-250 | 52.51 | 9.36 | 0.26 |
| X-350 | 60.02 | 10.71 | 0.26 |
| X-450 | 64.34 | 6.54 | 0.15 |
| X-550 | 75.04 | 0.27 | 0.005 |
| X-900 | 76.41 | 0.01 | 0.0002 |

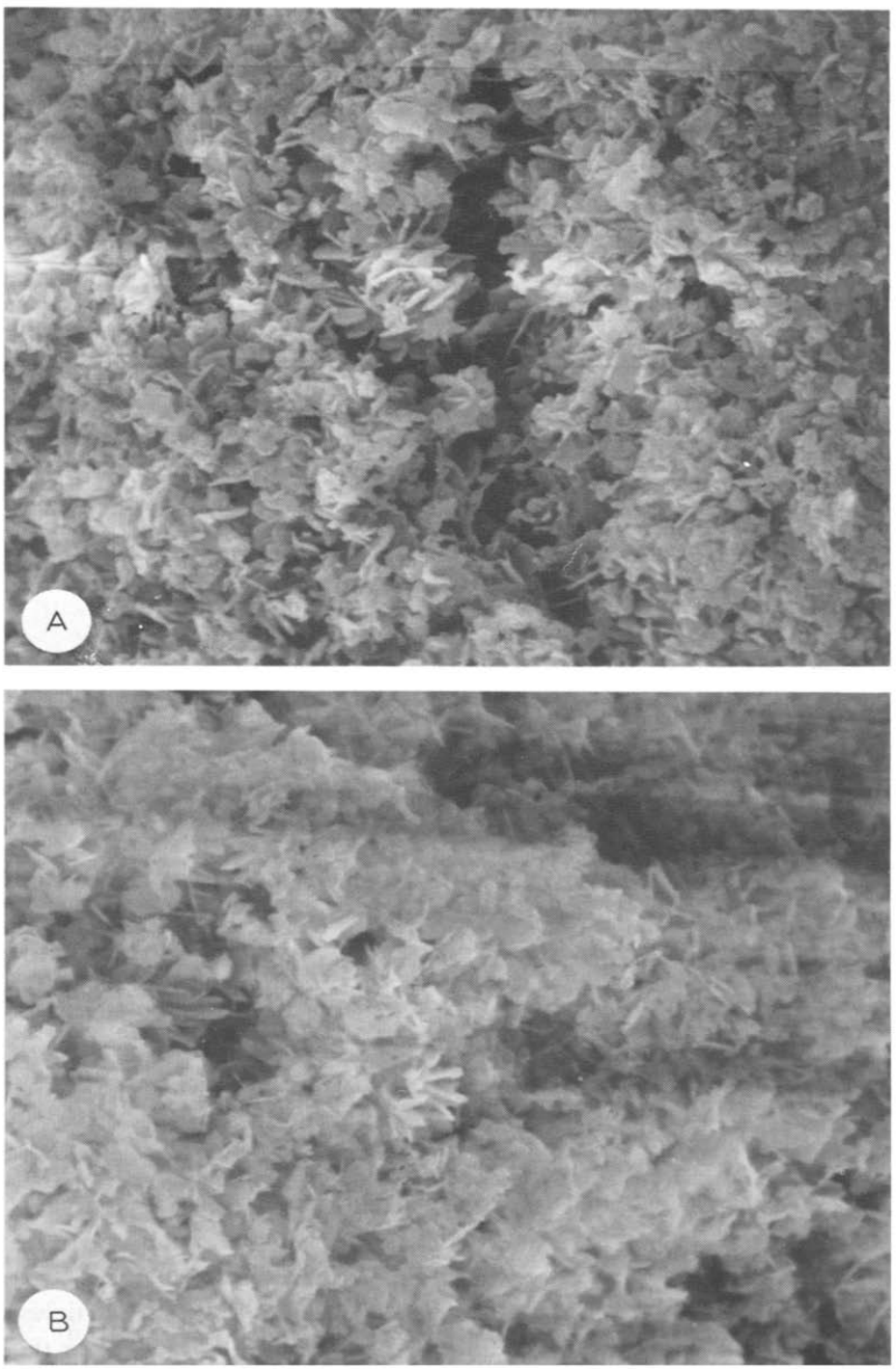


Fig. 2. SEM pictures of (A) the original sample and (B) calcined (1000°C, 1 h) powders; magnification 5000×.

curve are the results of the dehydration process, while the third one corresponds to the release of nitrogen compounds from the precipitates.

The X-ray diffraction patterns of the original sample and calcined powders are

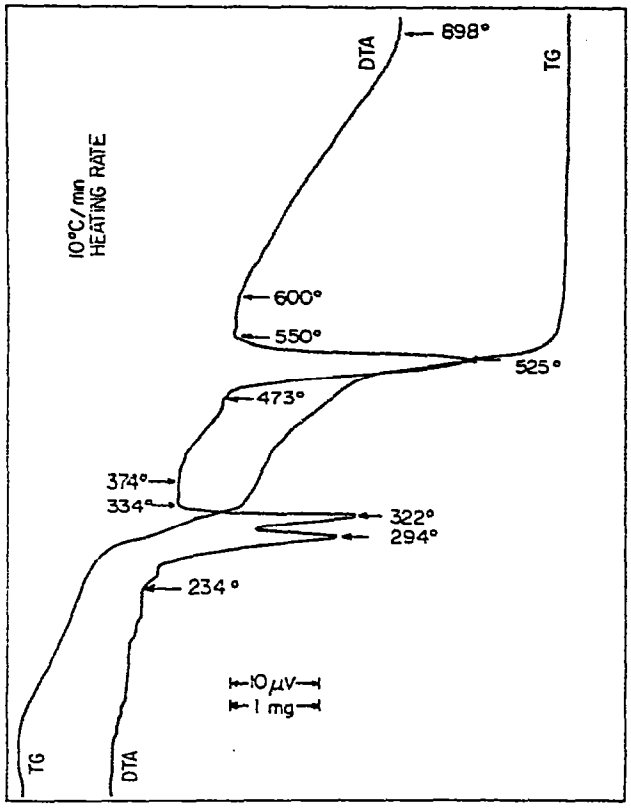


Fig. 3. DTA and TG curves of yttrium hydroxide nitrate powders. Each sample is about 20 mg.

shown in Fig. 4. At 250°C, the pattern (B) remained about the same as that of the original (A). When the sample was heated up to 350° and then 450°, different patterns (C and D) appeared, indicating different structures. By 550°, yttrium oxide became the only compound. At 900°, the peaks were sharper, resulting from the crystallite growth of $Y_2O_3$.

*Powder characterization*

*Specific surface area*

The specific surface area of calcined powders is shown in Fig. 5. Generally speaking, the surface area is at its highest value right after the decomposition reaction. As both temperature and time increase, the surface area decreases as a result of crystal growth and elimination of the pores within agglomerated particles.

At 560°, the sample (560-0), which was taken out of furnace immediately after the temperature reached the set point, did not have much of a chance to go through the decomposition reaction and therefore had only a small increase in surface area compared with the original value. Subsequent X-ray analysis of this sample also showed no existence of $Y_2O_3$. However, after one hour at 560°, the sample completed the decomposition reaction and increased its surface area to the highest value detected in this study.


Fig. 4. X-Ray diffraction patterns of A, the original sample; calcined samples: B, at 250°C; C, 350°C; D, 450°C; E, 550°C and F, 900°C.

In the study of the reduction of surface area during the initial stage in the sintering of ceramic powders and catalyst, an empirical equation of the form

$$(S_0/S)^{n-1} - 1 = S_0^{n-1}(n-1)k_1(t - t_0) \quad (1)$$

is often used [13,14]. In this equation, $S_0$ is the surface area of the sample taken out right after the temperature reached the desired value and $t_0$ is the corresponding "equivalent" time.

When the data set of this study was tested on eqn. (1), it was found that there

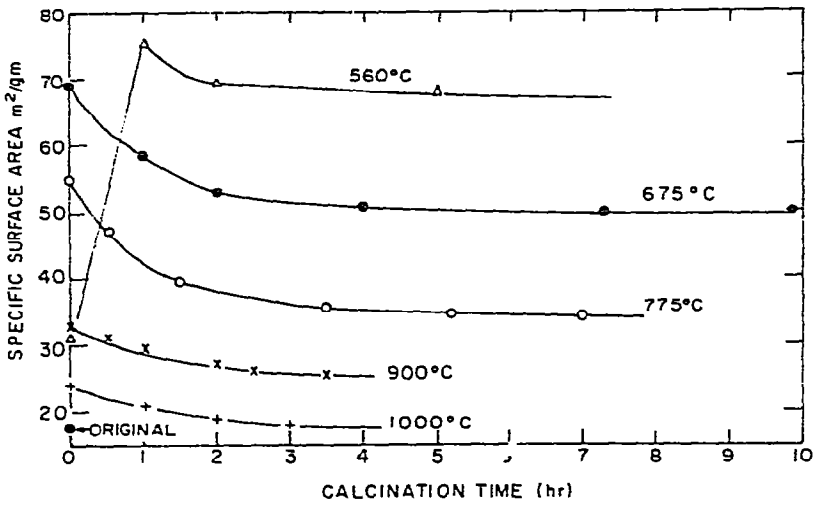


Fig. 5. Effects of calcination temperature and time on surface area.

existed a wide range of $n$ values which gave reasonably good correlation coefficients by the least squares method. Thus, it is very difficult to decide on $n$-values based on the results of fitness only. This fact shows that a different equation is needed to describe the kinetics of surface area reduction for the calcination of agglomerated powders.

*Particle size distribution*

From Fig. 6, we can see that as the calcination temperature increased, the effect of heat broke up the agglomerates and thus resulted in smaller mean diameters. However, as time progressed, the effect of sintering set in. Bridges presumably

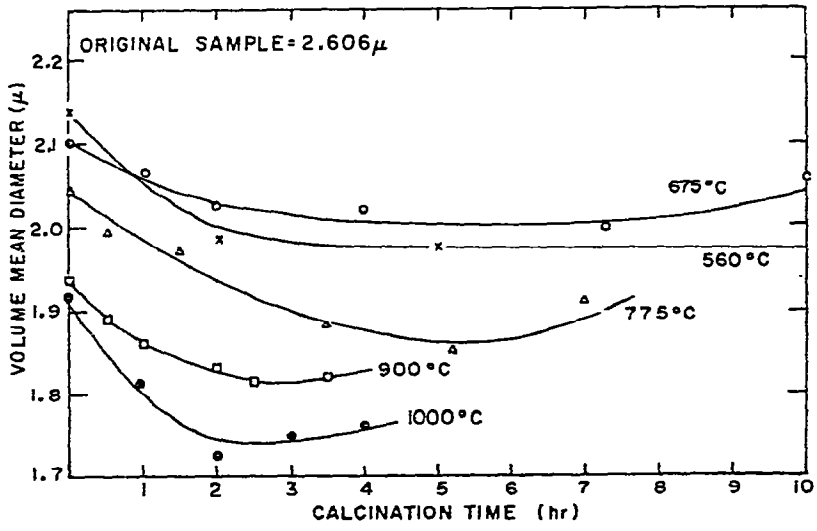


Fig. 6. Variation of mean particle size with respect to calcination temperature and time.

developed among adjacent crystallites and small agglomerates and as a result, the mean diameter increased.

*Pore volume distribution*

The changes in pore volumes with respect to temperature are shown in Fig. 7. For the sample 560-0, the decomposition had not yet finished and the volume increase of small pores was limited. At 675°, the reaction was completed and a large number of small pores were created. As the temperature continued to increase, the sintering effect began to eliminate the small pores and thus caused the size of the smallest pore at subsequent temperatures to increase. However, at the same time, the shrinkage of the crystallites began to create relatively large pores clearly shown in the case of 900-0.

*X-Ray crystallite size*

The crystallite size, as measured by the X-ray line broadening technique, is often used in the study of calcination and sintering [2,5,15,16]. The kinetic curves of crystallite growth from the present study are shown in Fig. 8.

When $\ln(D - D_0)$ is plotted against $\ln(t - t_0)$ (the measured calcination time, in minutes) for this case, straight lines of different slopes were obtained for different temperatures. If these slopes were evaluated by the Arrhenius equation, an empirical equation

$$D - D_0 = 10(t - t_0)^p \tag{2}$$

was then obtained where $p = 75 \exp(-10.8 \text{ kcal}/RT \text{ mole})$. Even though the fitness test of this equation is very good, the physical significance of this approach requires more detailed study.

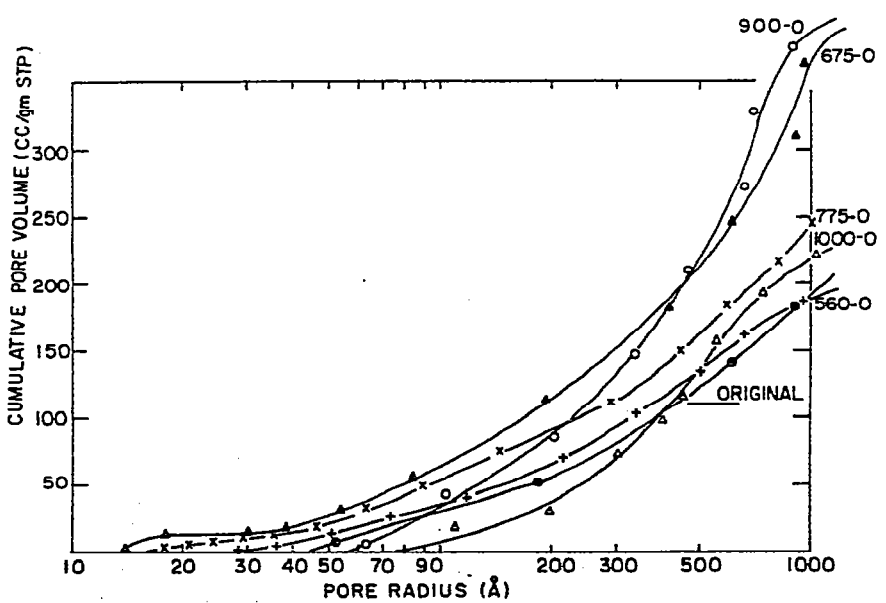


Fig. 7. Cumulative pore volume distributions of original and calcined powders.

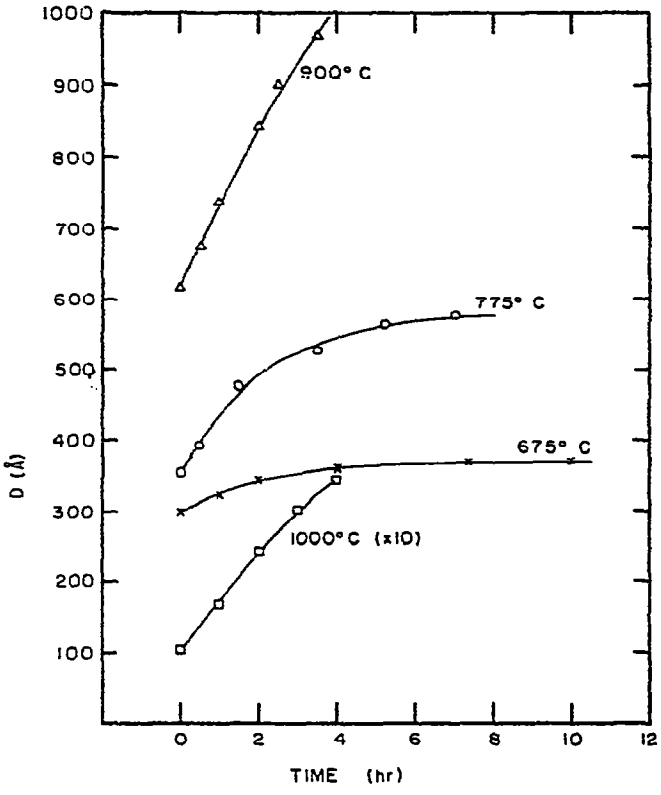


Fig. 8. Kinetic curves of X-ray crystallite size at different temperatures.

*Conversion (or crystallization)*

Data for the degree of conversion were tested according to different kinetic models for solid state reactions and transformations listed by Hulbert [17] and Jacobs [18]. Through trial and error, it was found that the Avrami–Erofeev equation of nucleation and growth concept produced the best fit (Fig. 9). The derived empirical equation has the form

$$\ln[(1-x_0)/(1-x)] = 0.60 \exp(-8000 \text{ cal}/RT \text{ mole}) \ (t-t_0)^{0.675} \qquad (3)$$

where $x_0$ was the initial conversion, corresponding to $t_0$ in min.

According to Christian [19], one-dimensional diffusion controlled growth could produce a time exponential of less than one in the Avrami–Erofeev equation. This seems to be consistent with the fact that the precipitate of yttrium hydroxide nitrate has a plate-like shape, i.e. one of its dimensions is much shorter than the other two. When this compound decomposes upon heating, an amorphous yttria is probably formed first, which then quickly nucleates and grows into very small crystallites.

In the theory of nucleation and growth controlled transformation, the conversion rate first goes through an induction period and then increases rapidly before it decreases to zero [19]. The results obtained in this study clearly correspond to the final stage of the transformation, showing decreasing conversion with time.

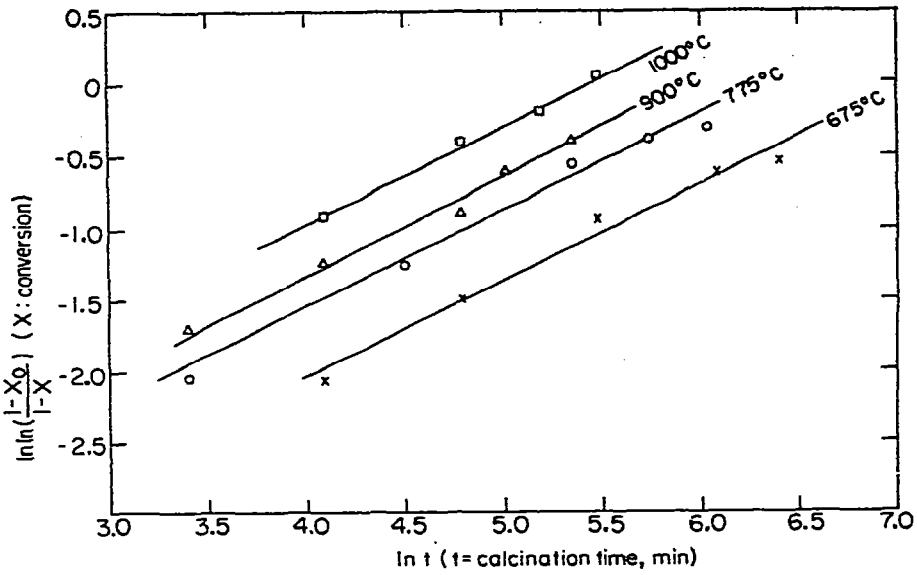


Fig. 9. Correlation of the degree of conversion by the Avrami–Erofeev equation.

*Relationship between properties of calcined powders*

*X-Ray crystallite size and specific surface area*

It has been suggested that a relationship of the form "$SD$ = constant" exists between crystallite size and specific surface area [20,21]. But when ln $S$ is plotted

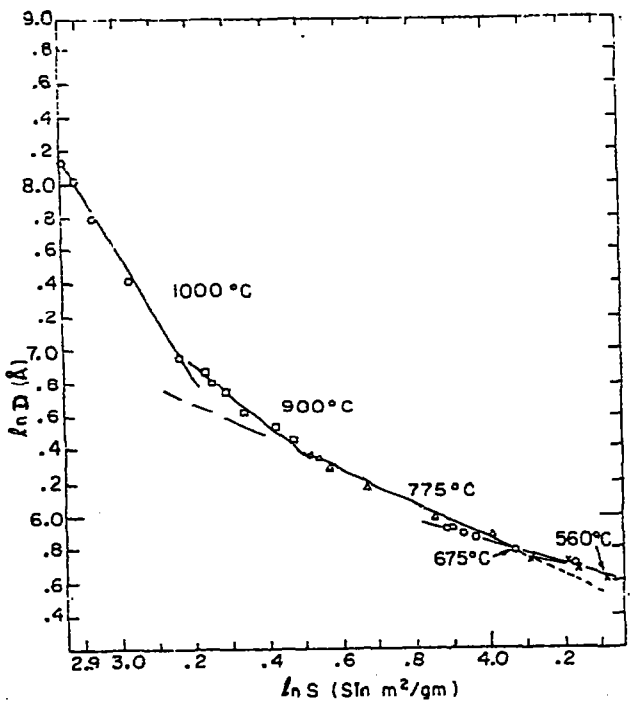


Fig. 10. Correlation between the specific surface area and X-ray crystallite size

against ln $D$ in Fig. 10, the slopes showed an increase with respect to temperature. In other words, the reduction in surface area is greater than the increase in X-ray crystallite size at higher temperatures. This can easily be explained by the fact that the majority of the powders are agglomerates, or very porous particles. As the calcination temperature increases, there are losses in surface area not only due to the increase in crystallite size, but also due to the sealing of pores.

*Conversion and crystallite size*

Upon completion of the last calcination reaction, amorphous yttria begins to convert into the crystalline form. Along with the increase in the degree of conversion, the size of crystallite also increases. Conceivably, both increases involve the same diffusion process. However, the crystallite can not only grow by converting neighboring amorphous regions into existing crystallites. It also grows by coalescing crystallites. When $\ln[1/(1-x)]$ is plotted against ln $D$ (Fig. 11), linear relationship of different slopes was obtained for 675 − 900°C and 1000°C. In that figure, we can see clearly that the growth rate of crystallite with respect to conversion at 1000° is higher than that for the 675–900° runs. It seems to suggest that the coalescing rate jumps to a higher level at this temperature.

Another observation of Fig. 11 shows that the last three points of the 675° series and the last point of the 775° series deviate below the straight line of $1-x = 560/D^{1.4}$. This might be explained by the existence of residual nitrate ions, which will obviously retard the growth of crystallites. As the calcination temperature increases, the amount of nitrate ion in the sample decreases and so does the retardation effect on the growth of yttria crystallites. Analysis of several calcined samples showed that there were 16, 9, 5, 2 ppm of residual nitrate ions in samples 675-10, 775-7, 900-3.5 and 1000-4, respectively.

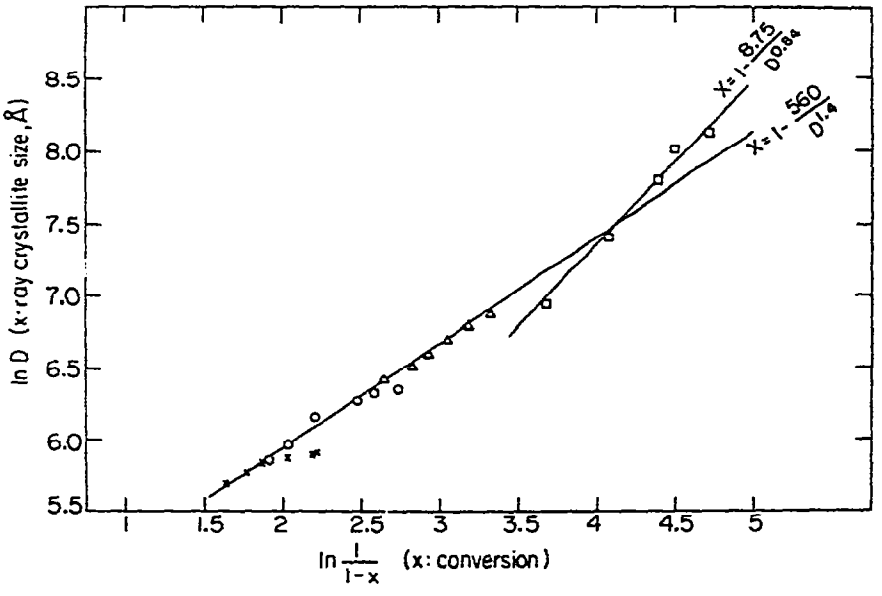


Fig. 11. Correlation between X-ray crystallite size and conversion.

ACKNOWLEDGEMENT

The authors wish to thank Mr. J.A. Herriott for his help in the measurement of specific surface area and pore volume distribution. This work was supported by the Basic Research Division, Department of Energy under contract No. W-7405-eng-82.

REFERENCES

1 D.T. Livey, B.M. Wanklyn, M. Hewitt and P. Murry, Trans. Br. Ceram. Soc., 56 (1957) 217.
2 A.W. Hey and D.T. Livey, Proc. Br. Ceram. Soc., 3 (1965) 13.
3 M.Y. Farah and S.A. El-Fekey, Acta Chim. Acad. Sci. Hung., 85 (1975) 383.
4 E. Crucean and D. Rand, Trans. J. Br. Ceram. Soc., 73 (1979) 58.
5 K.J.D. Mackenzie and P.J. Melling, Trans. J. Br. Ceram. Soc., 73 (1974) 23.
6 L.E. Burkhart, R.C. Hoyt and T. Oolman, Mater. Sci. Res., 13 (1979) 23.
7 S.L. Dole, R.W. Scheidecker, L.E. Shiers, M.F. Bernard and O. Hunter, Jr., Mater. Sci. Eng., 32 (1978) 277.
8 H.P. Klug and L.E. Alexander, X-Ray Diffraction Procedures for Polycrystalline and Amorphous Materials, Wiley, New York, 2nd edn., 1973, pp. 618–708.
9 E.A. Rosauer and R.H. Handy, Proc. Iowa Acad. Sci., 68 (1961) 357.
10 J.M. Haschke, Inorg. Chem., 13 (1974) 1812.
11 J.M. Haschke, J. Solid State Chem., 14 (1975) 238.
12 C.E. Holcombe, C.C. Edwards and D.A. Carpenter, Report Y-2104, Oak Ridge Y-12 Plant, Jan. 1978.
13 R.M. German and Z.A. Munir, Mater. Sci. Res., 10 (1975) 249.
14 J.T. Richardson, J.R. Crump and R.U. Osterwalder, Mater. Sci. Res., 13 (1979) 551.
15 M.J. Bannister, J. Am. Ceram. Soc., 58 (1975) 10.
16 U.D. Allred, S.R. Buxton and J.P. McBride, J. Phys. Chem., 61 (1957) 117.
17 S.F. Hulbert, J. Br. Ceram. Soc., 6 (1969) 11.
18 P.W.M. Jacobs, 4 (1969) 37.
19 J.W. Christian, The Theory of Transformation in Metals and Alloys. Part I. Experimental and General Kinetic Theory. Pergamon Press, Oxford, England, 1975.
20 W.S. Brey, Jr. and B.H. Davis, J. Colloid and Interface Sci. 70 (1978) 10–17.
21 A.N. Prabhn and R.W. Vest, 10 (1975) 399.